
Dynamic and Static ^{99m}Tc -ECD SPECT Imaging of Subacute Cerebral Infarction: Comparison with ^{133}Xe SPECT

Kuniaki Ogasawara, Akira Ogawa, Masayuki Ezura, Hiromu Konno, Mamoru Doi, Kiyoshi Kuroda, and Takashi Yoshimoto

Department of Neurosurgery and High-Technology Medical Research Center, Iwate Medical University, Morioka; Department of Intravascular Neurosurgery, Kohnan Hospital, Sendai; and Department of Neurosurgery, Tohoku University School of Medicine, Sendai, Japan

^{99m}Tc -ethylcysteinate dimer (^{99m}Tc -ECD) SPECT imaging reportedly fails to show reflow hyperemia in patients with subacute stroke. This study attempts to determine the clinical usefulness of dynamic ^{99m}Tc -ECD SPECT in evaluating regional blood flow in subacute cerebral infarction and the kinetic behavior of ^{99m}Tc -ECD in infarct areas. **Methods:** ^{133}Xe and consecutive dynamic and static ^{99m}Tc -ECD SPECT studies were performed on 24 patients with cortical infarction in the middle cerebral artery territory 13–15 d after the onset of a stroke. Image contrast between infarct and contralateral control areas on ^{99m}Tc -ECD tomograms (ECD uptake ratio) was compared with that on cerebral blood flow (CBF) images obtained using ^{133}Xe inhalation (CBF ratio). **Results:** In all cases, ECD uptake ratios from static images were lower than CBF ratios. This tendency was obvious when CBF in the infarct area increased above the normal control value, and no significant correlation was found between ECD uptake ratios from static images and CBF ratios. Only in the infarct areas with CBF below the normal control value, however, was a significant correlation between the two maintained ($r = 0.795$; $P = 0.0011$). A very strong correlation was found between CBF ratios and ECD uptake ratios on both the first dynamic scan (36 s after injection) ($r = 0.991$; $P < 0.0001$) and the second dynamic scan (72 s after injection) ($r = 0.945$; $P < 0.0001$). The correlation coefficient decreased in a time-dependent manner, with no significant correlation observed after the fourth dynamic scan (144 s after injection). On the other hand, significant correlations were observed on all dynamic scans only in the infarct areas with CBF below the control value. **Conclusion:** Super-early images of dynamic ^{99m}Tc -ECD SPECT provide a close imaging contrast with CBF and reveal reflow hyperemia in areas with irreversible changes produced by subacute stroke, which static ^{99m}Tc -ECD SPECT images fail to show. Decreased retention of the tracer in the infarct areas with hyperperfusion causes an underestimation of CBF on static ^{99m}Tc -ECD SPECT images. Given these results, we believe that dynamic ^{99m}Tc -ECD

SPECT is an effective clinical tool to evaluate regional blood flow in subacute cerebral infarction.

Key Words: ^{99m}Tc -ECD; subacute stroke; brain SPECT

J Nucl Med 2001; 42:543–547

In clinical practice, ^{99m}Tc -ethylcysteinate dimer (^{99m}Tc -ECD), developed as a retained-type brain perfusion tracer, has been widely used to visualize regional blood flow in the human brain with SPECT (1). Although the distribution of ^{99m}Tc -ECD in the brain correlates with regional cerebral blood flow (CBF) in healthy humans and in patients with chronic stroke (2–5), ^{99m}Tc -ECD SPECT imaging reportedly fails to show reflow hyperemia in patients with subacute stroke (5,6). ^{99m}Tc -ECD is a lipophilic agent that penetrates the normal blood–brain barrier and is retained by conversion of lipophilic molecules into hydrophilic compounds. The tracer is hydrolyzed to polar metabolites by deesterification (1), and thus ^{99m}Tc -ECD activity is decreased in damaged brain tissue with normo- or hyperperfusion (4–9). On the other hand, SPECT imaging contrast 60 s after ^{99m}Tc -ECD injection that matches that of CBF images has been found only in the misery perfusion of brain ischemia and the luxury perfusion of acute herpes encephalitis (10,11).

This study attempts to determine the clinical usefulness of ^{99m}Tc -ECD SPECT with dynamic scanning in evaluating regional blood flow in subacute cerebral infarction and the kinetic behavior of ^{99m}Tc -ECD in infarct areas.

MATERIALS AND METHODS

Patients

Twenty-four patients (10 women, 14 men; age range, 39–78; mean age \pm SD, 58 ± 11 y) admitted to Kohnan Hospital between June and December 1994 with subacute cerebral infarction associated with cerebral embolism were enrolled in the study (Table 1). At Kohnan Hospital, the first choice of treatment for cerebral embolism is local intra-arterial thrombolysis using recombinant

Received Jul. 5, 2000; revision accepted Dec. 11, 2000.

For correspondence or reprints contact: Kuniaki Ogasawara, MD, Department of Neurosurgery, Iwate Medical University, 19-1 Uchimaru, Morioka, 020-8505 Japan.

TABLE 1
Patient Clinical Data

Patient no.	Age (y)	Sex	Occlusion*	Interval from onset to SPECT (d)
1	77	M	Left ICA	14
2	39	M	Right MCA	14
3	57	M	Right MCA	15
4	61	M	Right MCA	13
5	61	F	Left MCA	13
6	50	M	Right MCA	14
7	59	M	None	14
8	63	M	None	13
9	66	F	Right MCA	14
10	46	M	Right MCA	15
11	78	F	Left ICA	15
12	55	F	Right MCA	14
13	48	F	Right MCA	14
14	40	M	Right MCA	15
15	53	M	Left MCA	14
16	64	F	Right MCA	13
17	47	M	None	13
18	50	F	None	14
19	52	M	Left ICA	15
20	65	M	Right MCA	14
21	68	F	Left MCA	14
22	73	F	Right MCA	15
23	54	M	None	14
24	74	F	Right MCA	14

*Angiographic finding.

ICA = internal carotid artery; MCA = middle cerebral artery.

tissue plasminogen activator. Treatment selection is based on three criteria: the patient has been hospitalized within 6 h of onset; no hypodensity is observed on a CT scan on admission; and occlusion is present in the middle cerebral artery (MCA). All patients who do not meet these criteria receive only conservative systemic care. To avoid inducing a deterioration of hemorrhagic transformation caused by delayed recanalization, we never administer medication that may affect the function of thrombocytes or the coagulation–fibrinolysis system. Mannitol or glycerol is administered for ischemic brain edema or hemorrhagic transformation. When this treatment is ineffective and brain herniation progresses, mild hypothermia or decompressive hemicraniotomy is performed. Thus, the subjects of this study did not meet our criteria for local intra-arterial thrombolysis and did not require mild hypothermia or decompressive hemicraniotomy.

Cerebral angiography was performed within 24 h of the onset of symptoms in all patients. Three patients presented with occlusions in the internal carotid artery and 16 presented with occlusions in the MCA. Angiographic occlusions were not evident in 5 patients. CT scans or MR images obtained 1 wk after the onset of the stroke revealed massive cortical infarction in the MCA territories of all patients.

Informed consent was obtained from all patients or their next of kin, and the study was approved by the ethics committee of Kohnan Hospital.

SPECT Imaging

A SPECT study was performed on all patients 13–15 d after the onset of stroke. SPECT images were obtained using a multidetector ring-type scanner, consisting of 64 NaI crystals in a 38-cm-diameter circle in the detector array. After tomographic reconstruction, the spatial resolution and slice thickness in the center of the plane were 9 and 16 mm, respectively, with full width at half maximum (FWHM) for static imaging and 20 and 25 mm FWHM for dynamic imaging. The energy window in this study was 140 keV ($\pm 15\%$). Projection data for static and dynamic imaging were processed using Ramachandran's filtered backprojection after the introduction of a Butterworth prefilter. A 64×64 (^{99m}Tc -ECD static) or 32×32 (^{99m}Tc -ECD dynamic and ^{133}Xe) image matrix was used.

Patients were administered the tracer in a quiet, dimly lit room while resting with their eyes open. The patient's head was immobilized with a ready-made plastic head holder so that the bilateral external auditory meatus were aligned to the machine-indwelling positioning crossed-light beam. To reproduce the same head position for all SPECT studies, three markers were affixed on the head under the guidance of a light beam. Of the three markers, two were placed on the anterior edge of the bilateral external auditory meatus, and one was placed on the midline of the nose ridge. The three markers lay along a plane perpendicular to the axis of camera rotation.

Patients inhaled 1,480 MBq ^{133}Xe gas for 1 min, and sequence SPECT imaging was performed every minute for 10 min using a high-sensitivity collimator. Quantitative CBF maps were reconstructed using the Kanno–Lassen method (12). ^{99m}Tc -ECD was prepared from a commercially supplied kit that contained no radioactivity, and [^{99m}Tc]pertechnetate was obtained from a molybdenum–technetium generator. Fifteen minutes after obtaining the ^{133}Xe SPECT scan, each patient received an intravenous bolus injection of ~ 900 MBq ^{99m}Tc -ECD. Dynamic scanning with a high-sensitivity collimator was started simultaneously and continued for a total of 288 s (eight scans) with a scan-time duration of 36 s. Static SPECT imaging with a high-resolution collimator proceeded 10 min after the tracer injection. Tomographic data were obtained continuously over a 20-min period (Fig. 1).

From among the axial slices, we selected one through the basal ganglia and then visually and manually drew one 11.1-cm² region of interest (ROI) in the infarct area shown on CT scans or MR images. The control ROI was mirrored onto the contralateral side, and the same set of ROIs was used for all SPECT studies. Image contrast between infarct and contralateral control areas on ^{99m}Tc -ECD tomograms (ECD uptake ratio) was compared with that on CBF images using ^{133}Xe inhalation (CBF ratio).

Statistical Analysis

We determined correlations between various parameters by linear regression analysis and by computing regression equations and correlation coefficients. Statistical significance was set at $P < 0.05$.

RESULTS

The dynamic ^{99m}Tc -ECD SPECT images of a representative patient (patient 24) with cortical infarction in the right MCA territory showed that maximum brain activity of ^{99m}Tc -ECD was found on the second scan (72 s after injection), which provided a close imaging contrast with ^{133}Xe

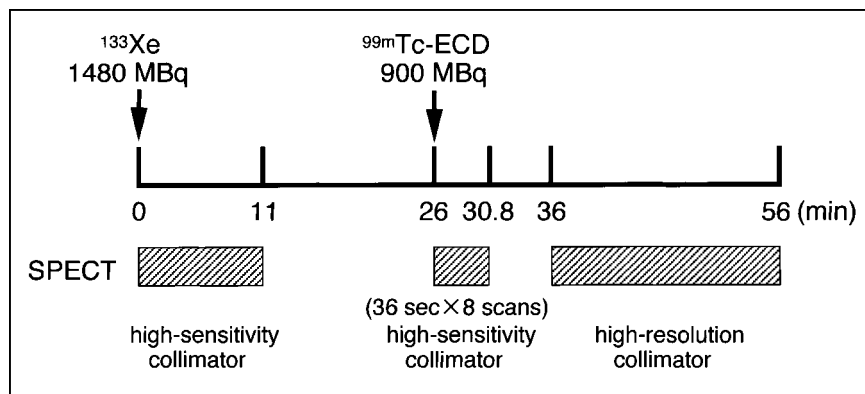


FIGURE 1. Protocol for consecutive ^{133}Xe and dynamic and static $^{99\text{m}}\text{Tc-ECD}$ SPECT imaging.

CBF; the activity in the contralateral control area was followed by some loss and a plateau, whereas that in the lesion decreased rapidly to below the activity in the contralateral area (Fig. 2). Static $^{99\text{m}}\text{Tc-ECD}$ SPECT revealed a focal area of hypoactivity corresponding to the lesion shown on the MR image.

ECD uptake ratios from static images were lower than CBF ratios from all infarct areas (Fig. 3C). This tendency was obvious when CBF in the infarct area increased above the mean value of the control group (46.1 mL/100 g/min) obtained from 10 healthy volunteers (age range, 35–65 y; mean age, 52.3 y). Although no significant correlation was found between ECD uptake ratios on static images and CBF ratios ($r = 0.109$), a significant correlation between the two was maintained ($r = 0.795$; $P = 0.0011$) just for the infarct areas with CBF below the mean value of the control group. A very strong correlation existed between CBF ratios and ECD uptake ratios on both the first dynamic scan (36 s after injection) ($r = 0.991$; $P < 0.0001$) and the second dynamic scan (72 s after injection) ($r = 0.945$; $P < 0.0001$) (Figs. 3A and B). In the infarct area with CBF greater than the mean value of the control group, ECD uptake ratios on the first dynamic scan were higher than CBF ratios. In contrast, ECD uptake ratios on the second dynamic scan fell below CBF ratios. The correlation coefficient decreased in a time-dependent manner, with no significant correlation observed after the fourth dynamic scan (144 s after injection) (Table 2). However, significant correlations were observed on all dynamic scans only in the infarct areas with CBF less than the mean value of the control group.

DISCUSSION

Our findings indicate that super-early images of dynamic $^{99\text{m}}\text{Tc-ECD}$ SPECT provide a close imaging contrast with CBF and reveal reflow hyperemia in areas with irreversible changes produced by subacute stroke that static $^{99\text{m}}\text{Tc-ECD}$ SPECT images fail to show. We also showed that decreased retention of the tracer in infarct areas with hyperperfusion causes an underestimation of CBF on static $^{99\text{m}}\text{Tc-ECD}$ SPECT images.

Flow tracer accumulation in the brain is influenced by various regulating factors depending on the scan time after tracer injection. In the super-early phase of tracer injection, the first-pass extraction fraction greatly affects brain tracer distribution. When the fraction of the tracer extracted from the blood into the brain is high and rapid scanning is sufficient to obtain the initial slope of the brain tracer input, the image is close to CBF (10). Thus, we hypothesized that even in subacute infarction, scanning in the super-early phase after a $^{99\text{m}}\text{Tc-ECD}$ injection is influenced negligibly by a complicated interaction of factors such as the backdiffusion of tracer from the lipophilic component in the brain to the blood or metabolic products in the blood. The results of our study show that super-early images within 2 min after intravenous injection of $^{99\text{m}}\text{Tc-ECD}$ provide a close imaging contrast with CBF in patients with subacute stroke.

However, on the first dynamic images, ECD uptake ratios were higher than CBF ratios in infarct areas with hyperperfusion. Radioactivity in arterial blood of $^{99\text{m}}\text{Tc-ECD}$ administered intravenously as a bolus injection reaches a maximum at 1 min after injection, which is followed by a steep decrease and a plateau at about 5 min after injection (4). Most of the tracer is present in the intravascular compartment at 30 s after injection. Regions of subacute cerebral infarction exhibit increased cerebral blood volume because of vasoparalysis or vasodilatation associated with metabolic acidosis (13). Therefore, the first dynamic images of $^{99\text{m}}\text{Tc-ECD}$ would overestimate CBF as a result of the cerebral blood pool effect of the tracer in the infarct area.

In contrast, the second dynamic image of $^{99\text{m}}\text{Tc-ECD}$ SPECT underestimated CBF in the infarct area with hyperperfusion. This tendency became more obvious in a time-dependent manner, and the correlation coefficient between ECD uptake ratios and CBF ratios decreased. As a result, dynamic images at 3 min after injection did not reveal regional blood flow. On the other hand, linearity between ECD uptake ratios and CBF ratios was observed on all dynamic images and even on static images only in the

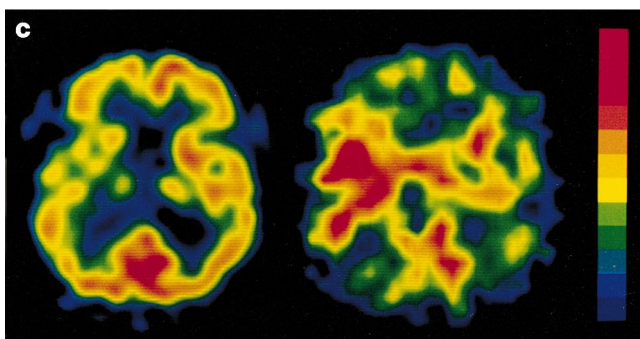
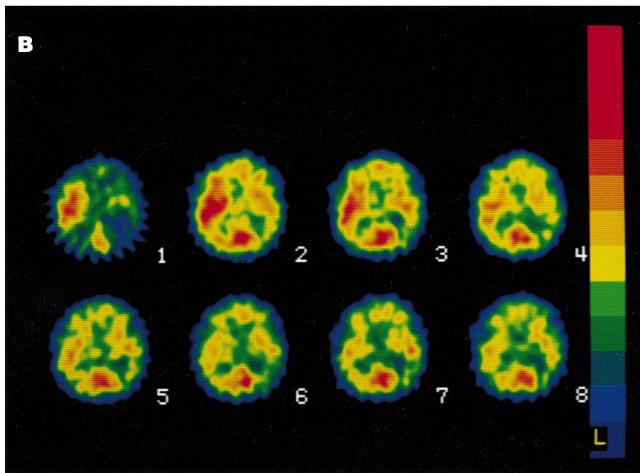
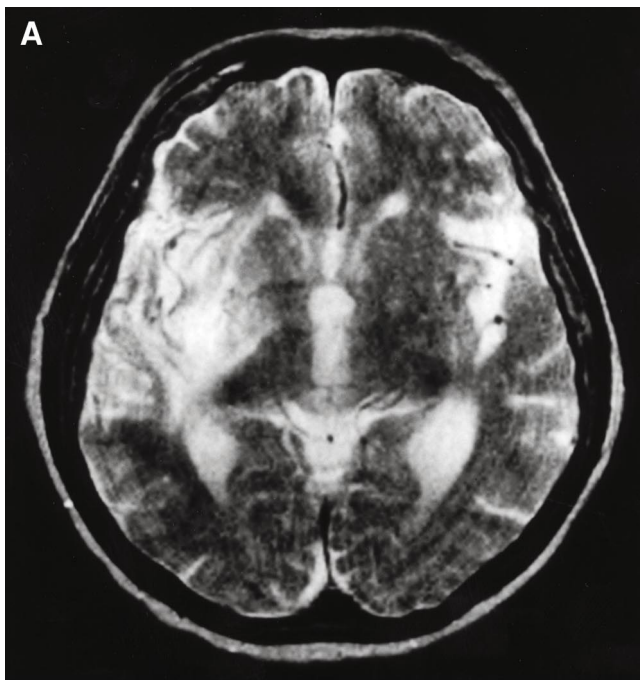


FIGURE 2. Patient 24. (A) T2-weighted MR image obtained 7 d after onset of initial symptoms reveals infarction in right MCA territory. (B) Dynamic ^{99m}Tc -ECD SPECT images show increased tracer concentration in infarct area in second scan (72 s after injection). Thereafter, ^{99m}Tc -ECD activity in lesion rapidly decreases to below that in contralateral area. (C) Static ^{99m}Tc -ECD SPECT image (left) shows focal hypoactivity corresponding to lesion detected on MRI. Same region shows marked hyperperfusion on ^{133}Xe tomogram (right).

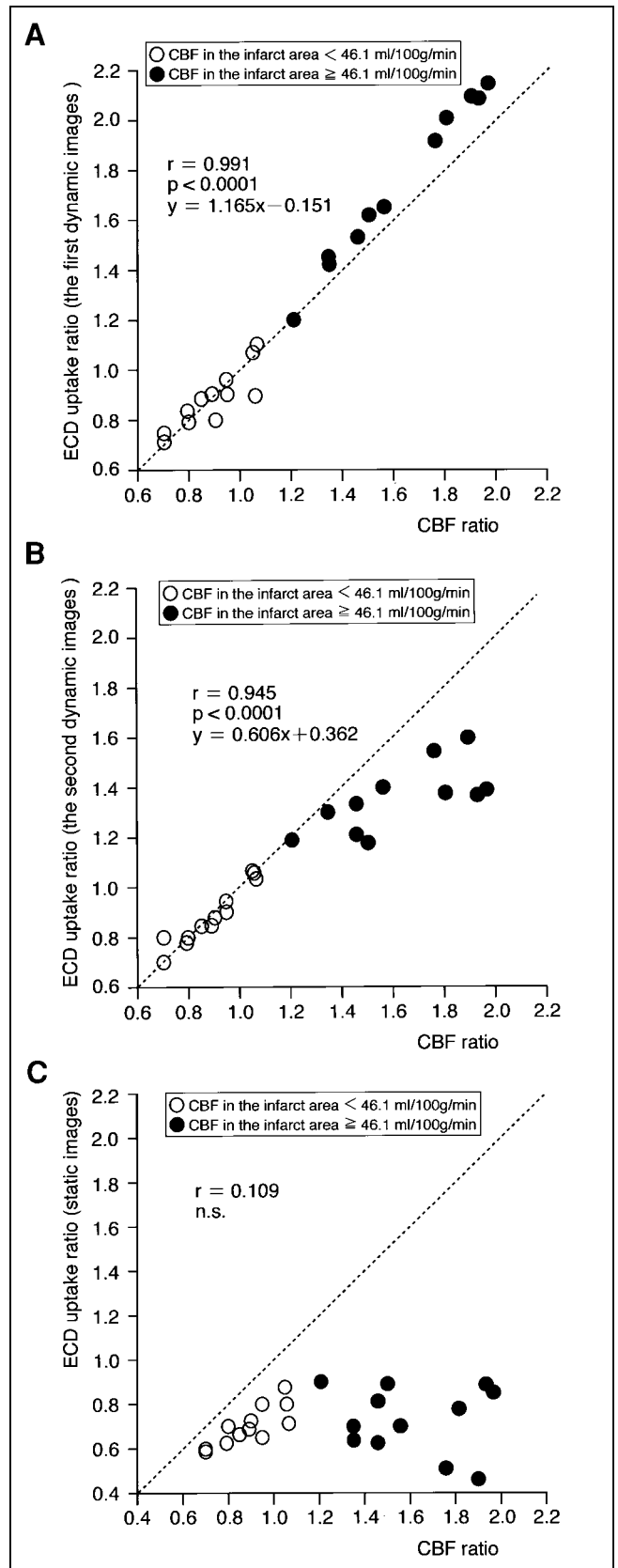


TABLE 2

Relationship Between ECD Uptake Ratios and CBF Ratios

SPECT scan time after tracer injection (s)	All infarct areas		Infarct areas with CBF below mean value of control group*	
	Correlation coefficient	P	Correlation coefficient	P
36	0.991	<0.0001	0.910	<0.0001
72	0.945	<0.0001	0.954	<0.0001
108	0.754	<0.0001	0.886	<0.0001
144	0.513	0.0094	0.803	0.0009
180	0.372	NS	0.754	0.0032
216	0.290	NS	0.731	0.0052
252	0.206	NS	0.711	0.0076
288	0.148	NS	0.705	0.0085

*Control group = 10 healthy volunteers.
NS = not significant.

infarct areas without hyperperfusion. ^{99m}Tc-ECD, transformed by intracellular esterases from a diester to a diacid complex, cannot cross the intact cell membrane and is trapped in the neural cell (1,14). Thus, the retention of ^{99m}Tc-ECD in the damaged brain depends on various factors such as the severity of blood-brain barrier breakdown and cytosolic esterase activity (10,11). Our findings suggest that hyperperfusion in infarct areas is more strongly related to decreased retention of ^{99m}Tc-ECD in patients with subacute stroke than any other factor. Furthermore, although static ^{99m}Tc-ECD SPECT images may provide a mix of information that reflects blood-brain barrier breakdown, cerebral metabolism, and CBF, our findings also suggest that static ^{99m}Tc-ECD SPECT images reveal regional blood flow in infarct areas without hyperperfusion.

In recent years, the development of a multihead gamma camera with high sensitivity and spatial resolution has made the measurement of regional CBF during low brain radioactivity possible. This measurement should enable super-early SPECT images to be obtained routinely in many institutions in the near future.

FIGURE 3. Relationships between relative ^{99m}Tc-ECD activity and relative CBF on first dynamic images (36 s after injection) (A), second dynamic images (72 s after injection) (B), and static images (C). Strong linearity between relative ^{99m}Tc-ECD activity and relative CBF is observed in first and second dynamic images. In infarct area with CBF > 46.1 mL/100 g/min, relative ^{99m}Tc-ECD activity on first dynamic scan exceeds relative CBF. In contrast, relative ^{99m}Tc-ECD activity in second dynamic scan is lower than relative CBF. Correlation between these in static images is not significant, whereas significant correlation is observed only in infarct areas with CBF < 46.1 mL/100 g/min. Dashed line represents line of identity. n.s. = not significant.

CONCLUSION

In areas with irreversible changes produced by subacute stroke, super-early dynamic ^{99m}Tc-ECD SPECT images provided a close imaging contrast with CBF and revealed reflow hyperemia, which static ^{99m}Tc-ECD SPECT images failed to show. Decreased retention of the tracer in the infarct areas with hyperperfusion caused an underestimation of CBF in static ^{99m}Tc-ECD SPECT images. Given these results, we believe that dynamic ^{99m}Tc-ECD SPECT is an effective clinical tool to evaluate regional blood flow in subacute cerebral infarction.

ACKNOWLEDGMENT

This work was supported in part by Grants-in-Aid for Advanced Medical Scientific Research by the Ministry of Science, Education, Sports and Culture, Japan.

REFERENCES

1. Walovitch RC, Hill TC, Garrity ST, et al. Characterization of technetium-99m-L-ECD for brain perfusion imaging. Part I. Pharmacology of technetium-99m-ECD in nonhuman primates. *J Nucl Med.* 1989;30:1892-1901.
2. Leveille J, Botez MI, Taillefer R, Gagnon A, Douesnard JM, Lefebvre B. A clinical comparison of Tc-99m HMPAO and Tc-99m ethyl cysteinate dimer (ECD) in normal volunteers and patients as a brain perfusion imaging agent [abstract]. *J Nucl Med.* 1988;29(suppl):P844.
3. Devous MD, Leroy RF, Payne JK, Lorimer MK, Bonte FJ. Comparison of Tc-99m ECD to Xe-133 in the SPECT determination of regional cerebral blood flow in patients with mild perfusion abnormalities [abstract]. *J Nucl Med.* 1990;31(suppl):P817.
4. Shishido F, Uemura K, Murakami M, et al. Cerebral uptake of ^{99m}Tc-bicisate in patients with cerebrovascular disease in comparison with CBF and CMRO₂ measured by positron emission tomography. *J Cereb Blood Flow Metab.* 1994; 14(suppl 1):S66-S75.
5. Lassen NA, Sperling B. ^{99m}Tc-bicisate reliably images CBF in chronic brain diseases but fails to show reflow hyperemia in subacute stroke: report of a multicenter trial of 105 cases comparing ¹³³Xe and ^{99m}Tc-bicisate (ECD, Neuro-lite) measured by SPECT on the same day. *J Cereb Blood Flow Metab.* 1994; 14(suppl 1):S44-S48.
6. Nakagawara J, Nakamura J, Takeda R, et al. Assessment of postischemic reperfusion and diamox activation test in stroke using ^{99m}Tc-ECD SPECT. *J Cereb Blood Flow Metab.* 1994;14(suppl 1):S49-S57.
7. Shishido F, Uemura K, Inugami A, et al. Discrepant ^{99m}Tc-ECD images of CBF in patients with subacute cerebral infarction: a comparison of CBF, CMRO₂ and ^{99m}Tc-HMPAO imaging. *Ann Nucl Med.* 1995;9:161-166.
8. Tamagac F, Moretti JLM, Defer G, Weinmann P, Roussi A, Cesaro P. Non-matched images with ¹²³I-IMP and ^{99m}Tc-bicisate single-photon emission tomography in the demonstration of focal hyperaemia during the subacute phase of an ischaemic stroke. *Eur J Nucl Med.* 1994;21:254-257.
9. Moretti JLM, Tamagac F, Weinmann P, et al. Early and delayed brain SPECT with technetium-99m-ECD and iodine-123-IMP in subacute strokes. *J Nucl Med.* 1994;35:1444-1449.
10. Shimosegawa E, Hatazawa J, Aizawa Y, et al. Technetium-99m-ECD brain SPECT in misery perfusion. *J Nucl Med.* 1997;38:791-796.
11. Fazekas F, Roob G, Payer F, Kapeller P, Strasser-Fuchs S, Aigner RM. Technetium-99m-ECD SPECT fails to show focal hyperemia of acute herpes encephalitis. *J Nucl Med.* 1998;39:790-792.
12. Kanno I, Lassen NA. Two methods for calculating regional cerebral blood flow from computed tomography of inert gas concentrations. *J Comput Assist Tomogr.* 1979;3:71-76.
13. Cordes M, Henkes H, Roll D, et al. Subacute and chronic cerebral infarctions: SPECT and gadolinium-DTPA enhanced MR imaging. *J Comput Assist Tomogr.* 1989;13:567-571.
14. Jacquier-Sarlin MR, Polla BS, Slosman DO. Cellular basis of ECD brain retention. *J Nucl Med.* 1996;37:1694-1697.